J. Fluid Mech. (2002), *vol.* 469, *pp.* 317–342.
DOI: 10.1017/S0022112002001908 Printed in the United Kingdom

Langmuir circulations beneath growing or decaying surface waves

By W. R. C. PHILLIPS

Department of Theoretical and Applied Mechanics,
University of Illinois at Urbana-Champaign, Urbana, IL 61801-2935, USA
wrphilli@uiuc.edu

(Received 15 March 2001 and in revised form 3 May 2002)

The instability to longitudinal vortices of two-dimensional density-stratified temporally evolving wavy shear flow is considered. The problem is posited in the context of Langmuir circulations, LCs, beneath wind-driven surface waves and the instability mechanism is generalized Craik–Leibovich, either CLg or CL2. Of interest is the influence of non-stationary base flows on the instability according to linear theory. It is found that the instability is described by a family of similarity solutions and that the growth rate of the instability, in non-stationary base flows, is doubly exponential in time, although the growth rate reduces to exponential when the base flow is stationary. An example is given for weakly sheared wind-driven flow evolving in the presence of growing irrotational surface waves. Waves aligned both with the wind and counter to it are considered, as is the role of stratification. Antecedent to the example is an initial value problem posed by Leibovich & Paolucci (1981) for neutral waves in slowly evolving shear. Here, however, the waves and shear may grow (or decay) at rates comparable with the LCs. Furthermore the current here has two components: a wind-driven portion due to the wind stress applied at the free surface and a second due to the diffusion of momentum due to the wave-amplitude-squared free-surface stress condition. Using the case for neutral waves in non-stratified uniform shear for reference, it is found, in general, that growing waves are stabilizing while decaying waves are destabilizing to the formation of LCs, although the latter applies only for sufficiently large spanwise spacings and is subject to a globally stable lower bound. Decaying waves in the absence of wind can also be destabilizing to LCs. When the wind is counter to the waves, however, only decaying waves are unstable to LCs. Furthermore, while growing waves are stable to the formation of LCs in the presence of stable stratification, decaying waves are unstable in both aligned and opposed wind-wave conditions. Unstable stratification on the other hand, is destabilizing to LCs for all temporal waves in both aligned and opposed wind-wave conditions.

1. Introduction

Langmuir circulations, or LCs, are organized convective motions that form in the surface layer of oceans, lakes and ponds when winds of moderate strength blow over them. In each instance LCs manifest as a parallel series of counter-rotating vortices that more or less align with the wind (Langmuir 1938). Moreover, they act at the surface to concentrate flotsam, seaweed and air bubbles into clearly visible streaks or bands, with spacings ranging from a few millimetres (Kenney 1993) to several hundred metres (Plueddemann *et al.* 1996). Many attempts have been made to

explain LCs (see reviews by Leibovich 1983 and Gargett 1989), in part because they are apparently ordered structures that arise from disorderly environments, but also because they are thought to be largely responsible for the formation of thermoclines and the maintenance of mixed layers in lakes and oceans. Indeed, in view of the importance of the mixed layer and the heat, mass and momentum transport processes therein (see e.g. Li, Zahariev & Garrett 1995), the notion of modelling LCs with a view to their inclusion in future global change models is compelling.

Of the suggested range of models to explain LCs, the most plausible have as their basis a nonlinear interaction between surface gravity waves and a weak current; and of interest here is the prevailing theory in this category, that of Craik & Leibovich (1976). These authors provide a rational derivation of a set of equations – the CL-equations – thought to govern LCs, given an $O(\epsilon^2)$ rotational mean current and an irrotational wave field of wave slope $O(\epsilon)$.

Interestingly, the CL-equations predict that activity akin to Langmuir circulations may result from either of two instability mechanisms, CL1 or CL2. CL1 requires a surface wave field with a high degree of spatial structure, whereas CL2 acts without special spatial structure (Craik 1977; Leibovich 1977), and is thus of particular relevance in the open ocean (see § 4). In consequence CL2 has formed the basis of numerous studies concerned with LCs, and the effect on them of stratification, nonlinearity and streamwise growth (e.g. Leibovich & Paolucci 1980, 1981; Leibovich, Lele & Moroz 1989; Cox *et al.* 1992; Cox & Leibovich 1993, 1997; Li & Garrett 1993, 1997; Skyllingstad & Denbo 1995; McWilliams, Sullivan & Moeng 1997; Phillips 2001*b*, henceforth referred to as Pb, and others).

Meanwhile test cases for such theories have resulted from an extensive observational program of ocean LCs (Thorpe & Hall 1982; Weller *et al.* 1985; Smith, Pinkel & Weller 1987; Weller & Price 1988; Zedel & Farmer 1991; Smith 1992, 1998; Plueddemann *et al.* 1996; Plueddemann & Weller 1999; Weller & Plueddemann 1996 and others). But although CL2-theory can account for some field observations (see e.g. Pb), studies employing it have, to this point, assumed neutral waves, whereas the waves in field studies on occasion grow or decay. For example, Plueddemann *et al.* (1996) report an instance where LCs are sustained by slowly decaying waves for tens of hours after an abrupt reduction in the local wind stress. Thus the focus of the present work is to explore the role growing or decaying waves play in the formation of LCs.

In such instances the Stokes drift is a function of time and, in the context of CL2 (which is described kinematically in § 2.1), has two components: one aligned with the direction of wave propagation and the second normal to the free surface. Of course unsteadiness of the primary wave field or base flow usually implies that the linear instability problem is non-separable and our first task is to explore that condition here. In doing so, however, we do not restrict attention to $O(\epsilon^2)$ shear and the CL-equations. Rather we take a more general view, noting that LCs form in a variety of levels of shear both in the laboratory and the ocean (Melville, Shear & Veron 1998). In consequence we begin with Andrews & McIntyre's (1978) generalized Lagrangian mean (GLM) formulation. This is an exact theory of nonlinear waves on a Lagrangian-mean flow in which the nonlinear wave–wave interaction is represented as a rectified effect through the $O(\epsilon^2)$ Stokes drift.

The CL-equations, of course, follow from GLM (Leibovich 1980), but relevant here are the CLg equations, an equation set intermediate between GLM and CL which allows for growing rotational or irrotational waves in any level of temporal shear (Phillips 1998, henceforth referred to as P98). The CLg-equations also recover two distinct regimes of CL-instability theory (see § 2): the strong-shear (Craik 1982*c*)

non-centrifugal (P98) version in which wave modulation is important, and Craik & Leibovich's (1976) aforementioned weak-shear centrifugal (Craik 1982*c*) version. Phillips (2003) denotes the former the generalized-CL, or CLg instability, while retaining the well-known CL2 notation for the latter; he further notes that CLg and CL2 are compact equivalents to the notations CL2-$O(1)$ and CL2-$O(\epsilon^2)$ introduced by Phillips, Wu & Lumley (1996).

Of particular interest is whether the CLg-equations are separable with non-stationary base flows, and we investigate this in § 3. Interestingly, not only are the equations separable, but the growth rate of the ensuing LCs described by them is doubly exponential in time, irrespective of the level of shear. The ensuing eigen-problem is, however, simplest when the shear is weak, and since this case has clear physical relevance to the open ocean, we consider it in detail in § 4. Specifically, we question the instability via CL2, of an evolving $O(\epsilon^2)$ shear layer in the presence of a temporal spanwise-independent Stokes drift field within the framework of an initial value problem introduced by Leibovich & Paolucci (1981, henceforth referred to as LP).

The paper is organized as follows: the CLg equations and similarity solutions to them are discussed in §§ 2 and 3, while a generalization of LP's initial value problem is posed in § 4 along with details of the primary fields, i.e. the mean Eulerian shear layer and mean Lagrangian (Stokes drift) fields. We then investigate the instability to LCs in neutrally stratified conditions: first in the presence of waves which propagate in the direction of the mean Eulerian velocity (§ 5) and then opposite to it (§ 6). The role of stratification is considered in § 7 and the results are discussed in § 8. Using the case of non-stratified uniform shear in the presence of neutral waves for reference, we find that growing waves are stabilizing and decaying waves destabilizing to CL2. We further find that while the instability is subject to a low-wavenumber cutoff when the waves grow, that is not the case when they decay. Finally, in accord with observation, we find that decaying waves in the absence of wind are destabilizing to CL2.

2. The generalized Craik–Leibovich instability

Following Craik (1982*c*), who restricted attention to inviscid shear flows with imposed neutral waves, P98 applied GLM to a class of temporal unidirectional viscous shear flows with imposed small-amplitude (rotational or irrotational) spanwise-independent growing waves. His intent was to remain general in regard to the level of the imposed shear and restrict only the maximum slope of the waves, *vis à vis* the instability of the ensuing wave–mean interaction to longitudinal vortices.

He thus considered the interaction between a unidirectional shear flow of characteristic velocity $\mathscr{V}$ and two-dimensional straight-crested waves of wavenumber α that propagate in the direction of the basic flow. The amplitude of the waves could grow from infinitesimal to finite, but their maximum slope ϵ must satisfy $\epsilon < O(1)$; since orbital velocities are then characterized by $\epsilon\mathscr{C}$, where $\mathscr{C}$ is a typical phase speed, the two velocity scales are usefully related by setting $\mathscr{V}/\mathscr{C} = O(\epsilon^s)$, where $s \geqslant 0$. Then by making variables dimensionless with respect to $\mathscr{C}$ and $\mathscr{L}$, where $\mathscr{L}$ is the characteristic thickness of the shear layer, the level of shear is also $O(\epsilon^s)$, and in the event viscosity plays a role, the Reynolds number $R \equiv \mathscr{L}\mathscr{C}/\nu_0$.

For clarity upper-case letters are used to denote primary flow quantities, which by design have no spanwise (y) dependence, with lower-case letters otherwise, while an overbar on an unscaled dimensionless variable denotes a streamwise average. Then with unit vectors $(\boldsymbol{i}, \boldsymbol{j}, \boldsymbol{k})$ in $\boldsymbol{x} = (x, y, z)$, the unperturbed Eulerian shear flow in the

reference frame of the waves is $\overline{\boldsymbol{U}}(z,t) = \epsilon^s[U,0,0]$ while the wave field is $\breve{\boldsymbol{U}}(x,z,t)$. Moreover if the wave field interacts with $\overline{\boldsymbol{U}}$ to excite streamwise-averaged Eulerian velocity perturbations $\tilde{\boldsymbol{u}}(y,z,t)$, whose strength relative to the primary shear flow is measured by the parameter Δ, the outcome, in GLM variables (see Andrews & McIntyre 1978), is the velocity associated vector field $\bar{\boldsymbol{q}} = \overline{\boldsymbol{Q}} + \tilde{\boldsymbol{q}}$, which is expanded as

$$\bar{\boldsymbol{q}}(y,z,t) = \epsilon^s\{[Q_1,0,\epsilon^{2-s}Q_3] + \Delta[q_1,\epsilon^n q_2,\epsilon^n q_3] + \cdots\} \quad (n \geqslant 0). \tag{2.1}$$

Correspondingly the wave–wave interaction produces $O(\epsilon^2)$ fields of pseudomomentum $\bar{\boldsymbol{p}}$ and Stokes drift $\bar{\boldsymbol{d}}$, which act to relate the Eulerian and Lagrangian mean velocity fields through $\bar{\boldsymbol{q}} = \bar{\boldsymbol{u}} + \bar{\boldsymbol{d}} - \bar{\boldsymbol{p}}$; in view of (2.1) the $\bar{\boldsymbol{p}}$ and $\bar{\boldsymbol{d}}$ fields are expanded as

$$\bar{\boldsymbol{p}}(y,z,t) = \epsilon^2\{[P_1,0,P_3] + \epsilon^s\Delta[p_1,\epsilon^n p_2,\epsilon^n p_3 + \cdots]\}, \tag{2.2}$$

where P_i result from the primary wave field and p_i represent modulations to it due to the evolving q_i field.

Evolution equations for the secondary flow then follow by substituting (2.1) and (2.2) into the GLM equations. We need not write the full set, but note that the key terms for CLg-type instabilities in the absence of viscosity necessitate (P98, equations (3.9) and (3.10))

$$\frac{\partial q_1}{\partial t} + \epsilon^2 D_3 \frac{\partial q_1}{\partial z} + \epsilon^{s+n} q_3 \frac{\partial Q_1}{\partial z} = 0 \tag{2.3a}$$

and

$$\frac{\partial \mathfrak{V}_1}{\partial t} + \epsilon^2 \frac{\partial}{\partial z}(D_3 \mathfrak{V}_1) + \epsilon^{2-n} \frac{\partial q_1}{\partial y}\frac{\partial P_1}{\partial z} - \epsilon^{s+2-n}\frac{\partial Q_1}{\partial z}\frac{\partial p_1}{\partial y} = 0, \tag{2.3b}$$

where

$$\mathfrak{V}_1 = \frac{\partial q_3}{\partial y} - \frac{\partial q_2}{\partial z}. \tag{2.3c}$$

Of interest are temporal secondary instabilities which lead to the growth of q_1 and $\mathfrak{V}_1$ with time due to z-differentiable wave–wave nonlinearities. Of course for other than algebraic growth the component equations (2.3a, b) must couple, and we should like to investigate that growth with coupling in the light of growing waves. First, however, a little background.

The CLg-equations (P98, equation (4.1)) follow from (2.3) when $n = (2-s)/2$. These describe in part (see Craik 1982c) the CLg instability, this being a wave-catalysed (McIntyre & Norton 1990), non-centrifugal (P98) instability that occurs in the presence of strong shear ($s = 0$) and rotational (or irrotational) waves that are subject to modulation owing to q_1. Wave modulation is absent in weak ($s = 2$) shear, however, and in this instance, and with irrotational waves, for which $\bar{\boldsymbol{p}} = \bar{\boldsymbol{d}} + O(\epsilon^4)$ (Andrews & McIntyre 1978), the CLg equations reduce to the CL equations. The latter, of course, describe the CL2 instability, which is a wave-catalysed, centrifugal instability. Phillips (2003) gives a thorough discussion of both the CLg and CL2 instabilities. Of course stratification may also play a role in the instability, so we now turn to the energy equation.

2.1. *The energy equation*

The CLg equations are rendered complete by an energy equation which accounts for rotational waves in all levels of shear. Since thermal effects were not considered by P98 and the CL-energy equation is restricted to irrotational waves and weak shear

(Leibovich 1977), we here derive a more general version. In accord with the CL version, however, we employ the Boussinesq approximation and replace density by temperature; we then write the streamwise-averaged dimensionless temperature as

$$\bar{\theta}(\boldsymbol{x}, t) = \theta_0(z) + \theta(\boldsymbol{x}, t),$$

where $\bar{\theta}(\boldsymbol{x}, t_0) = \theta_0(z)$ and $\theta(\boldsymbol{x}, t_0) = 0$ at some initial time $t = t_0$, With the usual approximations of thermal convection, the temperature is then governed by the energy equation which is, in GLM form,

$$\frac{\partial \theta}{\partial t} + \bar{\boldsymbol{q}} \cdot \nabla \theta = -\boldsymbol{k} \cdot (\bar{\boldsymbol{q}} + \bar{\boldsymbol{p}})\theta_0' + \kappa^* \nabla^2 \theta, \tag{2.4}$$

where a prime denotes $\mathrm{d}/\mathrm{d}z$ and the thermal diffusivity is $\kappa^* \mathscr{L}\mathscr{C}$.

As in P98, our intention is to isolate spanwise-independent primary fields and spanwise-dependent secondary fields, so on setting

$$\theta = \epsilon^2 \Theta(z, t) + \Delta \vartheta(y, z, t),$$

we find that the wave-induced evolution of the primary temperature field is described by

$$\frac{\partial \Theta}{\partial t} + \epsilon^2 Q_3 \frac{\partial \Theta}{\partial z} = -D_3 \theta_0' + \kappa^* \nabla^2 \Theta, \tag{2.5}$$

while the evolution equation for the secondary temperature field becomes

$$\frac{\partial \vartheta}{\partial t} + \epsilon^{s+n} \Delta \boldsymbol{q} \cdot \nabla \vartheta = -\epsilon^{s+n}(q_3 + \epsilon^2 p_3)\left(\theta_0' + \epsilon^2 \frac{\partial \Theta}{\partial z}\right) - \epsilon^2 Q_3 \frac{\partial \vartheta}{\partial z} + \kappa^* \nabla^2 \vartheta, \tag{2.6}$$

where $\boldsymbol{q} = [\epsilon^{-n} q_1, q_2, q_3]$.

Of course because $Q_3 = D_3 - P_3$ and $q_3 = w + \epsilon^2(d_3 - p_3)$, both neutral and irrotational waves render $Q_3 = 0$, the former because $P_3 = D_3 = 0$ (see § 3.1), the latter because $P_3 = D_3$ and $p_3 = d_3$. So if the waves are both neutral and irrotational, an initially isothermal primary temperature field Θ likewise bounded will remain so, in which case (2.6) reduces (for $s = 2$ and thus $\Delta = 1$ and with a rescaling in t as $\mathrm{t} = \epsilon^2 t$) to the form given by Leibovich. The Θ field will not, of course, remain unaltered if the waves (be they rotational or irrotational) grow in amplitude but, as evident from (2.6), such changes will not significantly influence the ϑ field because $\theta_0' = O(1)$.

2.2. *The role of growing waves*

Kinematically, CL2 (CLg) occurs because the Stokes drift gradient $\mathrm{D}D_1$ (irrotational portion of $\mathrm{D}P_1$), where $\mathrm{D} \equiv \partial/\partial z$, causes vortex lines to tilt forward wherever the Eulerian mean shear is distorted in y, giving rise to a longitudinal component of vorticity and ultimately vortices which, in the presence of neutral waves, grow (initially) exponentially fast. We might presume, therefore, that if CLg or CL2 is to be affected by temporal waves, then the above forcing is enhanced or diminished by an analogous term involving $\mathrm{D}D_3$; and such a term exists, as we see by expanding $\mathrm{D}(D_3 \mathfrak{V}_1)$. Indeed the component $-\partial q_3/\partial y \mathrm{D}D_3$ acts to counter or reinforce $-\partial q_1/\partial y \mathrm{D}D_1$, in accordance with the sign of $\mathrm{D}D_3$, since the components q_1 and q_3 are always in phase but of opposite sign.

But the vertical component of Stokes drift $S_3 = \epsilon^2 \mathscr{C} D_3$ represents, in the context of surface waves, the rate of change of the Lagrangian mean level of the water surface due to the rate of change of wave amplitude, the surface being elevated by an

$O((\epsilon/\alpha)^2)$ quantity (McIntyre 1988). Intuitively this quantity is small and whether S_3 can significantly influence the instability by the aforementioned mechanism (or other means) is decidedly unclear and must be resolved. Thus, in order to gain insight into the role played by S_3, irrespective of its magnitude, we first analyse the initial value problem for the formation of LCs via CLg, in the presence of growing waves.

3. Governing equations

As a starting point we note that temporal distributions of the Stokes drift and pseudomomentum are separable, at least for monochromatic waves, be they irrotational or rotational (Phillips 2001*a*, henceforth referred to as Pa). Separability is relevant here because it gives rise to the possibility that the initial value problem for the CLg-instability may reduce to a family of similarity solutions.

3.1. *Wave–wave nonlinearities*

The simplest example of Stokes drift of relevance occurs for two-dimensional irrotational monochromatic travelling waves of small amplitude which, with no loss in generality, we employ. S_1 is well known in this instance, but not S_3. Nevertheless S_3 can be deduced from Craik's (1982*b*) expressions for the generalized Stokes drift for monochromatic rotational waves or Pa's counterparts for broad spectra of temporal rotational waves. On setting $\mathscr{L} = \alpha^{-1}$, and thus $\mathscr{C}/\mathscr{L} = \sigma$, where σ is the wave frequency, both expressions reduce, for two-dimensional irrotational monochromatic waves, to

$$S_1 = \alpha\sigma a^2 \mathscr{A}^2(t) b\mathrm{e}^{2z} \quad \text{and} \quad S_3 = \alpha a^2 \mathscr{A}(t) \frac{\mathrm{d}\mathscr{A}}{\mathrm{d}t} b\mathrm{e}^{2z} \quad (-\infty < z \leqslant 0),$$

where a is a reference wave amplitude and $a\mathscr{A}(t)$ is the temporal wave amplitude, while b is a positive constant (set equal to 2 to concur with LP and Pb). Thus

$$S_1(z,t)/\mathscr{C} = \epsilon^2 D_1(z,t) = \epsilon^2 \mathscr{A}(t)^2 b\mathrm{e}^{2z} = \epsilon^2 B_1(t)\mathscr{D}_1(z) \tag{3.1a}$$

say, and

$$S_3(z,t)/\mathscr{C} = \epsilon^2 D_3(z,t) = \epsilon^2 \mathscr{A}(t) \frac{\mathrm{d}\mathscr{A}}{\mathrm{d}t} b\mathrm{e}^{2z} = \epsilon^2 B_3(t)\mathscr{D}_3(z), \tag{3.1b}$$

so that

$$\frac{S_3}{S_1} = \frac{D_3}{D_1} = \frac{B_3}{B_1} = O\left(\frac{1}{\sigma T_{gw}}\right) = O(\epsilon^{\mu}) \quad (\mu \geqslant 0), \tag{3.2}$$

say, where T_{gw} is the time scale for wave amplitude changes. Then $\mu > 0$ indicates that the waves grow on a scale which is long compared with σ^{-1}, which is reasonable physically.

3.2. *Similarity solution*

Since the scalings leading to (2.3) assume the dependent and independent variables are all $O(1)$ quantities we need not rescale them, but we do assume they are separable as

$$Q_1(z,t) = G(t)\mathfrak{Q}(z), \quad p_1(y,z,t) = C(t)\mathfrak{p}(y,z) \tag{3.3a}$$

and

$$q_i(y,z,t) = A_i(t)\mathfrak{q}_i(y,z) \quad \text{with} \quad \mathfrak{q}_i = [\mathfrak{u}, \mathfrak{v}, \mathfrak{w}], \quad \text{where} \quad i = 1,2,3; \tag{3.3b}$$

along with (3.1) and, since $A_2(t) \equiv A_3(t)$ by continuity,

$$\mathfrak{V}_1(y,z,t) = A_3(t)\left(\frac{\partial \mathfrak{w}}{\partial y} - \frac{\partial \mathfrak{v}}{\partial z}\right). \tag{3.3c}$$

Note that at this point we will not specify any relationship between $A_1(t)$ and $A_3(t)$, which means that q_1 and $\mathfrak{V}_1$, whose Eulerian counterparts represent streaks and LCs respectively, may grow at different rates.

Substituting (3.1) and (3.2) into (2.3) then yields

$$\kappa_{11}\mathfrak{u} + \epsilon^{2-s-n+\mu}\kappa_{12}\mathscr{D}_3\frac{\partial \mathfrak{u}}{\partial z} + \kappa_{13}\mathfrak{w}\frac{\mathrm{d}\mathfrak{Q}}{\mathrm{d}z} = 0 \tag{3.4a}$$

and

$$\kappa_{31}\left(\frac{\partial \mathfrak{w}}{\partial y} - \frac{\partial \mathfrak{v}}{\partial z}\right) + \epsilon^{n+\mu}\kappa_{32}\frac{\partial}{\partial z}\left\{\mathscr{D}_3\left(\frac{\partial \mathfrak{w}}{\partial y} - \frac{\partial \mathfrak{v}}{\partial z}\right)\right\} + \kappa_{33}\frac{\partial \mathfrak{u}}{\partial y}\frac{\mathrm{d}\mathscr{D}_1}{\mathrm{d}z} - \epsilon^{s}\kappa_{34}\frac{\partial \mathfrak{p}}{\partial y}\frac{\mathrm{d}\mathfrak{Q}}{\mathrm{d}z} = 0, \tag{3.4b}$$

where for self-similarity κ_{ij} are $O(1)$ constants such that

$$\kappa_{11} = \frac{\epsilon^{-(s+n)}}{GA_3}\frac{\mathrm{d}A_1}{\mathrm{d}t}, \qquad \epsilon^{\mu}\kappa_{12} = \frac{A_1B_3}{GA_3}, \qquad \kappa_{13} = 1 \tag{3.5a,b,c}$$

with

$$\kappa_{31} = \frac{\epsilon^{n-2}}{A_1B_1}\frac{dA_3}{dt}, \qquad \epsilon^{\mu}\kappa_{32} = \frac{A_3B_3}{A_1B_1}, \qquad \kappa_{34} = \frac{GC}{A_1B_1}, \qquad \kappa_{33} = 1. \tag{3.6a,b,c,d}$$

Observe that with a minor reformulation (as in § 4) and for specified κ_{12}, κ_{32} and κ_{34}, along with boundary conditions such as those used by Phillips & Wu (1994) for specific cases with $s = 0$, that (3.4) constitutes (with a further equation for $\mathfrak{p}$) an eigenvalue problem for κ_{11} and κ_{31}, not just when the waves are neutral but for growing waves as well. Moreover, while the A_i usually grow exponentially fast in separable problems of this type, that is the case here only when the wave field is neutral, as we shall see shortly. Finally, because κ_{12} and κ_{32} are zero as a consequence of (3.1*b*) only when the wave field is neutral and change sign according to whether the waves grow or decay, the steady states for (3.4) probably reflect distinct eigenbranches for growing, neutral and decaying waves; and in fact do, as we shall see in §§ 5, 6.

3.3. *Growth rates for the case $A_1 = A_3$*

Of particular interest are the growth rates for A_1 and A_3 and how they couple with the growth rate of the waves. To learn more of that coupling we turn to (3.6*b*) and use (3.2) to obtain

$$\frac{A_3}{A_1\mathscr{A}}\frac{\mathrm{d}\mathscr{A}}{\mathrm{d}\epsilon^{\mu}t} = \kappa_{32},$$

from which we find that

$$\ln \mathscr{A}(t) - \ln \mathscr{A}(t_0) = \kappa_{32}\int_{t_0}^{t}\frac{A_1}{A_3}\mathrm{d}(\epsilon^{\mu}t). \tag{3.7}$$

Of course the simplest case of interest is that for which $A_1 = A_3$, which occurs when the wave amplitude grows (or decays) exponentially fast, albeit as $\epsilon^{\mu}t$, via

$$\mathscr{A}(t) = \mathscr{A}(t_0)\exp\{\epsilon^{\mu}\kappa_{32}(t - t_0)\}, \tag{3.8}$$

in which case the temporal portions of our wave–wave measures become, from (3.1),

$$B_1(t) = \mathscr{A}^2(t_0)\exp\{2\epsilon^\mu \kappa_{32}(t-t_0)\} \quad \text{and} \quad B_3(t) = \epsilon^\mu \kappa_{32} B_1(t). \tag{3.9a,b}$$

Moreover we can use (3.9) in (3.6a) to find

$$A_1(t) = A_1(t_0)\exp\left\{\frac{\epsilon^{2-n-\mu}\kappa_{31}}{2\kappa_{32}}\mathscr{A}^2(t_0)[\exp\{2\epsilon^\mu\kappa_{32}(t-t_0)\}-1]\right\} \quad (\kappa_{32}\neq 0), \tag{3.10}$$

which decrees that growing or decaying wave fields excite doubly exponential growth. Note, however, that because κ_{32} is positive for growing and negative for decaying waves, that the amplitude A_1 will be significantly larger for growing than decaying waves after time t, all other things being equal. Of course on rewriting (3.10) (see (3.13)) to expose the influence of κ_{32}, we find that A_1 reverts to exponential growth for neutral waves, i.e. when $\kappa_{32}=0$, in accord with previous work.

It remains to determine $G(t)$ and $C(t)$: the first follows from (3.5a) as (see also § 3.4)

$$G(t) = \frac{\kappa_{31}}{\kappa_{11}}B_1(t), \tag{3.11}$$

while the latter follows from (3.5c) as

$$C(t) = \frac{\kappa_{34}\kappa_{11}}{\kappa_{31}}A_1(t). \tag{3.12}$$

Thus for self-similarity the primary shear flow must grow at the same rate as the Stokes drift, while modulation of the wave field due to the secondary flow (via q_1) must, as expected, occur at the same rate as the evolving secondary flow.

3.4. *Time scales and an eigen-problem*

Our task now is to gain some feel for the parameters s, n and μ and their interrelationship, and we do so by referring to the times scales that have so far entered the analysis. First, the requirement $\kappa_{i1} = O(1)$ $(i=1,3)$ necessitates we rescale time in (3.4a,b) as $t_1 = \epsilon^{s+n}t$ and $t_3 = \epsilon^{2-n}t$ respectively. Furthermore our restriction $A_1 = A_3$ necessitates that $t_1 = t_3 = \mathrm{t}$, say, and thus that $s = 2-2n$ (as noted previously by P98); it likewise decrees that the time scale over which LCs evolve is $T_{LC} = (\epsilon^{s+n}\sigma)^{-1}$. Second, as deduced earlier, the time scale over which surface waves evolve is $T_{gw} = (\epsilon^\mu\sigma)^{-1}$, so that

$$T_{LC} = \epsilon^{n+\mu-2}T_{gw}.$$

Thus if the LCs grow on a time scale that is equal to or faster than that of the waves, then $n+\mu \geqslant 2$.

Returning now to (3.4), we see that terms containing κ_{12} and κ_{32} are each premultiplied by $\epsilon^{n+\mu}$, while the term containing κ_{34}, which reflects wave modulation, is premultiplied by ϵ^s. Craik (1982c), in his work on CLg, notes that the $O(\epsilon^s)$ term needs to be retained only when $s=0$, because only then is wave modulation important. The terms premultiplied by $O(\epsilon^{n+\mu})$, on the other hand, are concerned with wave growth and it is appropriate to ask whether these terms too need be retained only when $n+\mu=0$? Interestingly Melville *et al.*'s (1998) laboratory experiments in $s=0$ shear do not realize $n+\mu=0$; rather they indicate $T_{gw} \approx T_{LC}$, suggesting $n+\mu=2$.

Nevertheless on rewriting (3.10) to reflect the role of κ_{32}, we find that

$$A_1(\mathrm{t}) = A_1(\mathrm{t}_0)\exp\{\kappa_{31}\mathscr{A}^2(\mathrm{t}_0)[(\mathrm{t}-\mathrm{t}_0)+\epsilon^{n+\mu-2}\kappa_{32}(\mathrm{t}-\mathrm{t}_0)^2+\mathrm{h.o.t.}]\} \tag{3.13}$$

and see that the growth of A_1 is affected not only by the eigenvalue κ_{31}, but also

by the growth or decay of the primary wave field through $\epsilon^{n+\mu-2}\kappa_{32}$. Indeed growing waves can significantly affect the growth of A_1, and thus the LCs. Thus since the influence of wave growth must be retained in (3.13) and affects the eigenstates, as we saw in § 3.2, it is necessary to likewise retain such terms in (3.4), even though $\epsilon^{n+\mu}$ may not be $O(1)$; see also § 4.2.

3.5. *The role of diffusion*

The inclusion of diffusive-like terms does not affect the separability of (2.3), but they do introduce the additional terms

$$\epsilon^{-s-n}R^{-1}\kappa_{15}\nabla^2\mathfrak{u} \quad \text{and} \quad \epsilon^{2-n}R^{-1}\kappa_{35}\nabla^2\left(\frac{\partial\mathfrak{w}}{\partial y}-\frac{\partial\mathfrak{v}}{\partial z}\right) \tag{3.14}$$

(in (3.4*a*, *b*) respectively), the parameter R and the further constraints

$$\kappa_{15}=\frac{\nu}{\nu_0}\frac{A_1}{A_3G} \quad \text{and} \quad \kappa_{35}=\frac{\nu}{\nu_0}\frac{A_3}{A_1B_1}. \tag{3.15}$$

So, with $A_1 = A_3$ as before, and purely viscous diffusion (i.e. $\nu/\nu_0 = 1$) then (3.15) are satisfied only when G and B_1 are constant. Physically this requires a stationary base flow and neutral waves, although Foster (1965), Homsy (1973) and Craik (1977) have deduced techniques that yield precise stability limits when the primary flow is unsteady.

But when the diffusion of momentum is primarily turbulent, and ν is interpreted as an eddy viscosity ν_T say, enforcement of (3.15) is (because ν_T is an approximation) secondary to that of other κ_{ij}, and it is reasonable to require only that κ_{15} and κ_{35} be constant over the time scales of integration. This approximation was invoked by LP and Pb, who set B_1 and ν_T constant while allowing G to evolve gradually with respect to the LCs. Of course to the same degree of approximation we could likewise allow B_1 to evolve at a rate comparable with G.

Alternatively, and with equal credibility from the view point of simplistic turbulence models, we could impose a spatially uniform eddy viscosity $\nu_t(t)$ that evolves at the same rate as the Stokes drift, say as

$$\frac{\nu_t(t)}{\nu_0}=B_1(t), \tag{3.16}$$

where ν_0 is a convenient reference eddy viscosity. Then, since $G \propto B_1$ from (3.11), all κ_{ij} are constant and our eigenvalue problem is valid for both stationary and non-stationary base flows. In short, it describes the initial evolution of LCs via CLg due to growing (or neutral) waves and evolving (or stationary) shear flows of all strengths. To be specific, the eigenvalue problem is defined by (3.4) and (3.14) with (3.5), (3.6) and (3.15), subject to boundary conditions such as those introduced in § 4.1 with the addition of a further equation to describe wave distortion when $s = 0$. The problem is thus simplest when $s \neq 0$ and we shall consider such a case in § 4.

4. An example: Langmuir circulations in weak shear

Of particular interest are LCs which form as a consequence of the dominant surface waves in the open ocean. In this instance the mean shear and the Stokes drift are of the same order (because the ocean surface velocity is ϵ^2 smaller than the wave phase velocity; see § 2) and because each is a montage of contributions from all wavenumbers (see e.g. Smith 1992; Pb), each may vary with y, z and t. However, provided the waves

comprise a continuous spectrum of wavenumbers of random phase, the Fourier components in the spanwise y-direction phase mix to zero (Craik & Leibovich 1976), rendering the Stokes drift spanwise independent. The relevant instability mechanism is then CL2. Furthermore, because the length scales associated with LCs are typically large compared with those of the energy-containing turbulent eddies in the ocean background, the ensuing large- and small-scale dynamics essentially decouple (see e.g. Phillips *et al.* 1996), so that turbulent diffusion of momentum may be reasonably modelled by an eddy viscosity. We now incorporate these features and the notions of LP to explore the influence on CL2 of growing or decaying waves.

4.1. *Background*

LP consider the formation of LCs via CL2 in an initially quiescent liquid which is subject to acceleration at its free surface. They take the view that the instability works its way down from the surface, following the imposition there of a wave field and a wind stress; the layer may then be thought of as infinitely deep and the shear within it to resemble a Rayleigh stress layer. Craik (1982*a*), however, notes that the shear layer is actually made up of two mean components: one arising from the diffusion of momentum due to the applied wind stress and a second due to the viscous diffusion of momentum due to the wave-amplitude-squared surface stress condition (see § 4.3). Indeed, because the second component and differential Stokes drift are always present in free-surface wavy flows, the flow is susceptible to destabilization by CL2 even in the absence of wind, a result consonant with Plueddemann *et al.*'s observations. Inclusion of the second component therefore not only enhances the physics in the model but further means that we can credibly allow for both growing and decaying waves, the former probably propagating in the direction of the wind, the latter in no wind, or propagating counter to it.

We thus extend LP's initial value problem to consider the formation of LCs beneath growing or decaying surface waves of characteristic slope $\epsilon \ll 1$, in the presence of stress-driven shear in deep water. Here the water is initially at rest and its temperature varies as $\theta_0(z)$. Then, at time $t = 0$, surface waves and a stress u_*, due both to the wind and induced viscous action of the waves, are imposed. The stress, which is aligned in the positive x-direction, provides the only source of external work. Furthermore, it causes the velocity in the substrate to grow and affects, either directly or indirectly, growth (or decay) of the wave field, which may propagate in either the positive or negative x-direction. The wind on the other hand, when present, propagates always in the positive x-direction. Finally, we set z positive vertically upwards and let the mean free surface coincide with the (x, y)-plane.

Because the waves are irrotational, $\bar{\boldsymbol{q}}$ contracts to its mean Eulerian form $\bar{\boldsymbol{u}}$, but in order to compare our results with those of LP and Pb it is necessary to recast the CLg equations discussed in §§ 2 and 3 in the manner of Leibovich (1977). Specifically, while retaining the above spatial and temporal scales as

$$\{[x, y, z]\alpha^{-1}, T_{LC}t\}, \tag{4.1}$$

but noting that t here is equivalent to t in § 3.4 with $T_{LC} = (\nu_0/\sigma)^{1/2}/a\alpha u_*$, the streamwise-averaged Eulerian mean and perturbation velocity components are here written as

$$\mathscr{C}[\overline{\boldsymbol{U}} + \tilde{\boldsymbol{u}}] = \left\{ [U(z,t) + u(y,z,t)]\mathscr{V},\ [v(y,z,t),\ w(y,z,t)]u_* a \left(\frac{\sigma}{\nu_0}\right)^{1/2} \right\}, \tag{4.2}$$

where $\mathscr{V} = u_*^2/\alpha v_0$. Further with $\mathrm{D} \equiv \partial/\partial z$, and temperature perturbations $\vartheta\alpha^{-1}\theta_0'$, the ensuing linear perturbation equations relative to the substrate $U(z,t)$ and linear thermocline $\theta_0(z)$ are, P98,

$$\frac{\partial u}{\partial t} = -w\mathrm{D}U - D_3\mathrm{D}u + La\nabla^2 u \tag{4.3a}$$

and

$$\frac{\partial \Omega}{\partial t} = -\mathrm{D}(D_3\Omega) - \frac{\partial u}{\partial y}\mathrm{D}D_1 + Ri\frac{\partial \vartheta}{\partial y} + La\nabla^2\Omega, \tag{4.3b}$$

where, since the wave field is irrotational,

$$\Omega = \mathfrak{V}_1 = \frac{\partial w}{\partial y} - \frac{\partial v}{\partial z}, \tag{4.3c}$$

with, from (2.6)

$$\frac{\partial \vartheta}{\partial t} = -w + LaPr^{-1}\nabla^2\vartheta, \tag{4.3d}$$

with $\nabla \cdot \boldsymbol{u} = 0$ where $\boldsymbol{u} = (u, v, w)$.

Three parameters enter (4.3): the Langmuir number La, the turbulent Prandtl number Pr (where κ_T is the eddy diffusivity of heat) and the Richardson number Ri, as

$$La = \frac{\alpha v_t}{au_*}\left(\frac{v_0}{\sigma}\right)^{1/2}, \qquad Pr = \frac{v_t}{\kappa_T}, \qquad Ri = \frac{v_t}{v_0}\frac{v_0}{\sigma}\frac{N^2}{(au_*\alpha)^2},$$

where $N^2 = \beta g\theta_0'$ is the Brunt–Väisälä frequency with β the thermal coefficient of expansion and g gravity.

Finally, to complete the initial value problem, we introduce the boundary conditions

$$\boldsymbol{k}\cdot\boldsymbol{u} = \mathrm{D}(\boldsymbol{u}\times\boldsymbol{k}) = \vartheta = 0 \quad \text{on} \quad z = 0, \tag{4.4a}$$

$$\boldsymbol{u} \to 0, \quad \vartheta \to 0 \quad \text{as} \quad z \to -\infty, \tag{4.4b}$$

the initial values

$$\boldsymbol{u}(\boldsymbol{x}, 0) = \boldsymbol{u}_0(\boldsymbol{x}), \qquad \vartheta(\boldsymbol{x}, 0) = 0 \tag{4.4c}$$

and the requirement that $\boldsymbol{u}_0(\boldsymbol{x})$ is solenoidal.

4.2. *Numerical formulation*

Prior to proceeding numerically, we rewrite (4.3) in a form that assumes the following: first, that the LCs are spanwise periodic with wavenumber l; second, since the substrate is a boundary layer, that the perturbations approach a constant value exponentially fast as $z \to -\infty$ (see Brown & Stewartson 1965; Phillips 1996); and third, in view of § 3, that the dependent variables are separable. We thus write

$$(\boldsymbol{u}, \vartheta) = A_1(t)[\hat{\boldsymbol{u}}(z), \hat{\vartheta}(z)]\mathrm{Re}\{\mathrm{e}^{\gamma z + \mathrm{i}ly}\} \tag{4.5}$$

(where $\gamma \geqslant 0$ is a constant) and, since the physical domain is semi-infinite, map to the finite plane with the transformation $\zeta = \mathrm{e}^z$, rendering $\mathrm{D} \equiv \zeta\partial/\partial\zeta$.

From § 3.2 and (4.3) we then have

$$\kappa_{11}\hat{u} = -\hat{w}\mathrm{D}\mathfrak{U} - \mathscr{D}_3^*(\mathrm{D}+\gamma)\hat{u} + La(\mathrm{M} - l^2)\hat{u}, \tag{4.6a}$$

$$\kappa_{13}(\mathrm{M}-l^2)\hat{w} = l^2\hat{u}\mathrm{D}\mathscr{D}_1 - \mathrm{D}[\mathscr{D}_3^*(\mathrm{M}-l^2)\hat{w}] + \gamma\mathscr{D}_3^*(\mathrm{M}-l^2)\hat{w} + La(\mathrm{M}-l^2)^2\hat{w} - l^2Ri\hat{\vartheta}, \tag{4.6b}$$

$$\kappa_{14}\hat{\vartheta} = -\hat{w} + LaPr^{-1}(\mathrm{M} - l^2)\hat{\vartheta}, \tag{4.6c}$$

where $\kappa_{14} = A_1^{-1}\mathrm{d}A_1/\mathrm{d}t$, with the operator

$$\mathrm{M} \equiv \zeta \frac{\partial}{\partial \zeta}\left(\zeta \frac{\partial}{\partial \zeta}\right) + 2\gamma\zeta \frac{\partial}{\partial \zeta} + \gamma^2$$

and boundary conditions

$$\frac{\partial \hat{u}}{\partial \zeta} + \gamma \hat{u} = \hat{w} = \frac{\partial^2 \hat{w}}{\partial \zeta^2} + (1+2\gamma)\frac{\partial \hat{w}}{\partial \zeta} + \gamma^2 = \hat{\vartheta} = 0 \quad \text{on} \quad \zeta = 1, \tag{4.7a}$$

$$\hat{u} = \hat{w} = \hat{\vartheta} = 0 \quad \text{with all derivatives bounded on} \quad \zeta = 0. \tag{4.7b}$$

Note that while (4.3*a*) and (4.3*b*) are together separable for both stationary and non-stationary base flows (see § 3), the inclusion of (4.3*d*), which accounts for thermal effects, restricts separability to stationary base flows, at least away from the linear steady states. This means that while no restrictions with regard to the respective growth rates of the LCs and waves apply to the eigenvalue problem defined by (4.6*a*), (4.6*b*) with $\kappa = \kappa_{11} = \kappa_{13}$, $Ri = 0$ and (4.7), its counterpart for $Ri \neq 0$ has similar ubiquity only for the linear steady states ($\kappa_{11} = \kappa_{13} = \kappa_{14} = 0$). So, since the purpose of this example is to ascertain the role of growing waves, we shall restrict attention when $Ri \neq 0$ (§ 7) to the linear steady states. Moreover, to accentuate the influence of wave growth, we assume in all cases that $\mathscr{D}_3^* = \epsilon^{\mu}\kappa_{12}\mathscr{D}_3 = O(1)$. We then study the instability at snapshots in the time evolution of the substrate velocity and waves.

Numerical solutions to (4.6) with (4.7) and $\mathscr{D}_3^* = 0$ are given by LP and Pb. Galerkin techniques were employed in both studies, although Pb used orthogonal basis functions while LP did not, which led to flawed results (for their $Ri \neq 0$ cases). LP also set $\gamma = 0$ while Pb used $\gamma = 1$. In addition to ensuring that the perturbation quantities in (4.5) have the correct asymptotic behaviour in the limit $z \to -\infty$, the value $\gamma = 1$ has the added advantage of rendering results insensitive to the choice of boundary conditions in that limit, because $\boldsymbol{u}$ and all derivatives of it with respect to z are homogeneous there.

Here the numerics resemble those of Phillips & Wu (1994) and Pb: specifically, the dependent variables $\hat{u}$, $\hat{w}$ and $\hat{\vartheta}$ are each expanded in linearly independent, complete sets of basis functions truncated after N terms. The eigenvalues $\kappa_{11} = \kappa_{13}$ are unkown. Substitution of the expansions into (4.6) and evaluation of the inner products then leads to a system of linear, homogeneous algebraic equations of the form $\kappa\mathbb{L} = \mathbb{M}$, where the elements of the matrices $\mathbb{L}$ and $\mathbb{M}$ are known from the inner products. The resulting eigenvalue problem was solved using LaPak with $N = 25$, and the code was validated by accurately reproducing other linear instability problems, for example the Dean problem (see Drazin & Reid 1981) and the thermohaline Rayleigh–Jeffreys problem (Baines & Gill 1969).

4.3. *Primary shear*

LP regard the $O(\epsilon^2)$ mean shear to be solely wind initiated through the wind stress at the surface, but it can, as Craik (1982*a*) notes, be just as readily attributed to the free-surface boundary condition, i.e. by the induced viscous action of the waves (Longuet-Higgins 1953). Specifically, if we suppose that a uniform wave field is rapidly set up at $t = t_0$ and that the waves are subsequently maintained at constant amplitude by suitable periodic normal stresses, then we may replace the wind stress in LP's analysis by the velocity gradient determined by the free-surface boundary condition. The velocity gradient is likewise determined if the surface is truly free

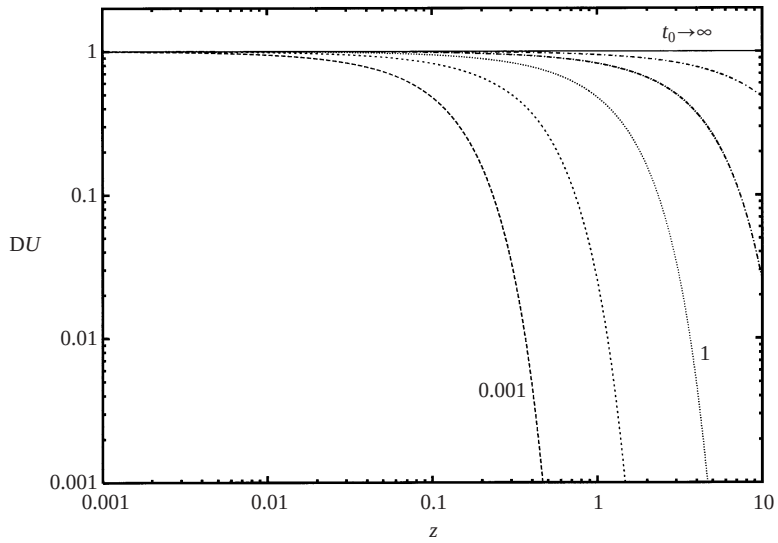

FIGURE 1. Gradients of the Eulerian mean velocity in accelerating laminar flow at $t_0 = 0.01$, 0.1, 1.0, 10.0, 100 and as $t_0 \to \infty$.

with no applied normal stresses, although then the wave amplitude decays owing to viscous action.

Here we allow for both a wind stress and a free-surface wave stress. However, rather than treating a plethora of cases we choose to employ a consistent set of base flows. Indeed, irrespective of the relative values of the wind stress and free-surface wave stress, we assume their (vector) sum is at all times constant (see §§ 5, 6). Physically this is a very severe restriction, because it requires that higher wind stresses be offset by a decrease in wave stress through a decrease in wave amplitude. Nevertheless it enables us to compare results from case to case and it is not at odds with our similarity solution.

Finally, in order to compare our results with those of LP and Pb, we assume the developing substrate shear $\mathrm{D}U(z,t)$ due to the constant stress u_*, is given always by a solution to the stress Rayleigh problem as $\mathrm{D}U(z,t) = \mathrm{erfc}(\eta)$ where $z = -2\eta(tLa)^{1/2}$. However, in order to comply with the separable form required in (4.6), we write near our initial time point of interest $t = t_0$, that

$$\mathrm{D}U = G(t)\mathrm{D}\mathfrak{U}(z) = G(t)\mathrm{erfc}(\eta_0), \quad \text{where} \quad \eta_0 = -\frac{z}{2(t_0La)^{1/2}}. \tag{4.8}$$

Equation (4.8) is plotted in figure 1 for various values of t_0, some of which, namely $t_0 = 0.01, 1$ and ∞, are used in the examples to follow.

4.4. *Wave amplitude*

We also require the dimensionless wave amplitude $\mathscr{A}$ as a function of the wave 'age' τ and determine it by first interpreting a (in § 3.1) as the maximum amplitude of the waves, so that the actual amplitude is $a\mathscr{A}(\tau)$. The non-dimensional amplitude $\mathscr{A}(\tau)$ is then subject to the requirements that it be unity when the waves are neutral and, if the waves are growing, that it satisfy $\mathscr{A}(\tau) \sim 0$ as $\tau \to -\infty$ and $\mathscr{A}(\tau) \sim 1$ as $\tau \to +\infty$; the obverse is the case if the waves are decaying. We shall not solve for $\mathscr{A}(\tau)$; rather

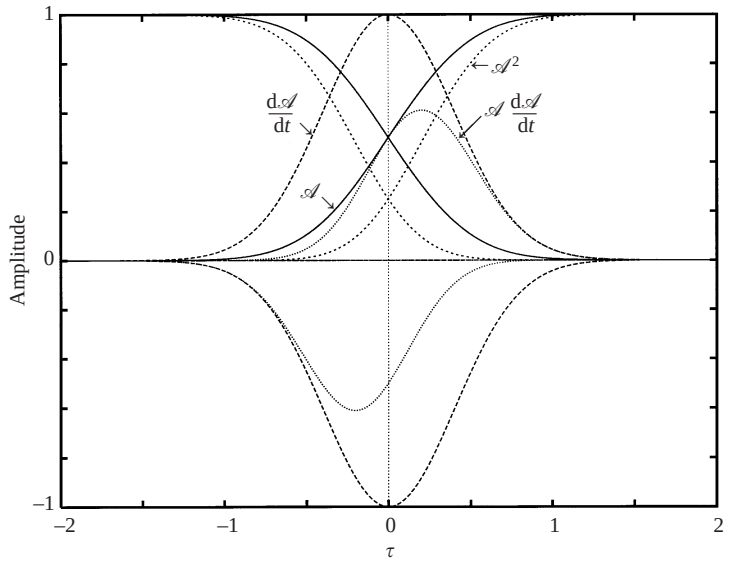

FIGURE 2. Sketch of the amplitude function $\mathscr{A}$ its gradient $\mathrm{d}\mathscr{A}/\mathrm{d}\tau$ and the products $\mathscr{A}^2$ and $\mathscr{A}\mathrm{d}\mathscr{A}/\mathrm{d}\tau$ for growing ($m = 1$) and decaying ($m = -1$) waves.

we assume it takes the form

$$\mathscr{A}(\tau) = \frac{1}{2}\left[2 - m^2 + \frac{m\tau}{|\tau|}\mathrm{erf}(H|\tau|)\right] \quad (-\infty < \tau < \infty), \tag{4.9}$$

where $m = [1, 0, -1]$, according to whether the waves are growing, neutral or decaying.

For convenience we set $H = \sqrt{\pi}$, so that $\mathrm{erf}(H) \approx 0.99$. Curves of $\mathscr{A}$, $\mathscr{A}^2$ and $\mathscr{A}\mathrm{d}\mathscr{A}/\mathrm{d}\tau$ are plotted in figure 2. Here we see for growing waves that $D_3 \approx 0$ when $\tau = -1$ while D_3 is a maximum near $\tau = 0.2$; likewise $D_3 \approx D_1$ when $\tau = 0.3$, while $D_1 \approx 2D_3$ when $\tau = 0.5$. Lastly, although $D_1(-0.5) \approx 0$, it transpires that $D_3(-0.5)$ while small is much greater than $D_1(-0.5)$. Similar cases exist for decaying waves, albeit with $D_3(\tau)$ replaced by $-D_3(-\tau)$ and so test cases were done at various $\tau = \tau_0$ values of interest, namely $\tau_0 = 0, \pm 0.2, \pm 0.3, \pm 0.5, \pm 1$.

Finally we note that the levels of maturity of the evolving shear flow and wave field are uncoupled. For example waves may be present because of some distant past weather event, while locally the wind speed might increase from zero. Alternatively the wind might increase from zero in otherwise quiescent conditions causing both the shear and waves to grow. In short the age of the shear t_0 and the age of the waves τ_0 (not to be confused with the wave 'age' used by oceanographers), are uncorrelated.

5. Aligned wind and waves

We begin by considering flows in which the wind and waves propagate in the same direction. In order to do so we note that because external work, accomplished by the application of suitable stresses, is required to maintain purely periodic waves in a viscous liquid, we take the view that the waves are neutral or grow only in the presence of a wind stress, and decay only in the absence of a wind stress. Then, in order to compare various cases, we require, as mentioned in §4.3, that the sum of the wind and free-surface wave stresses, remains constant. Rather than specify the proportions of each stress, however, we instead specify values of τ_0 and t_0. This then

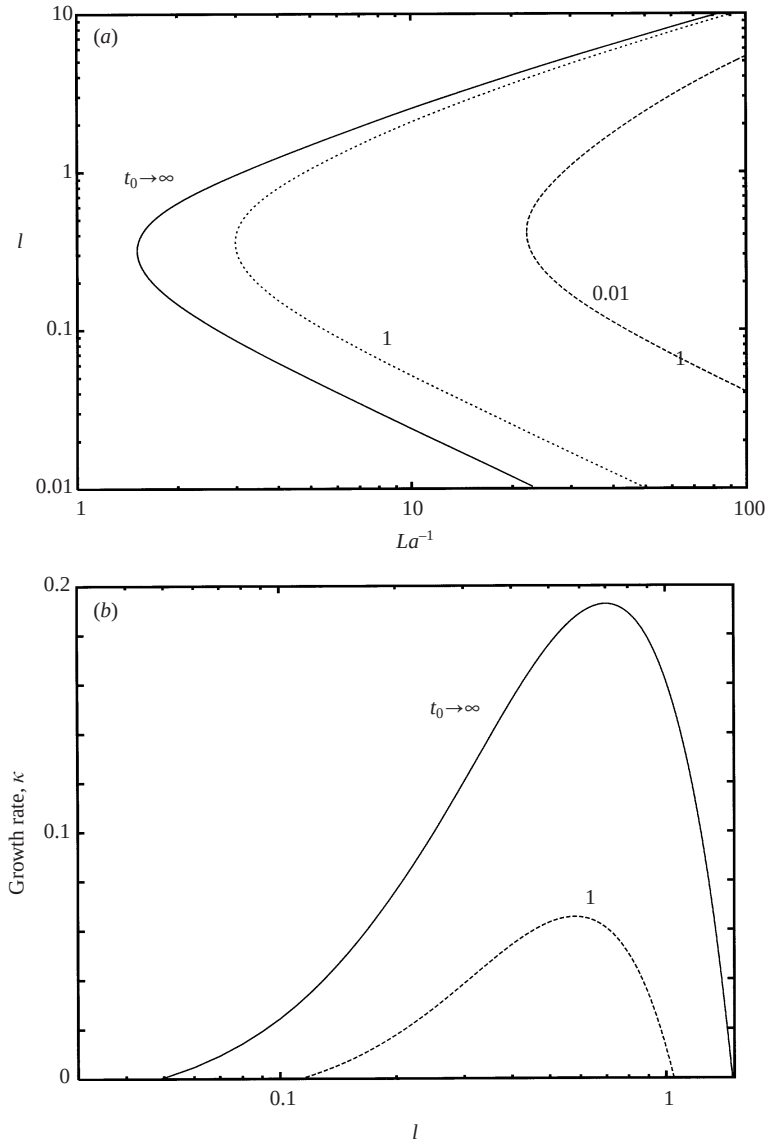

FIGURE 3. Developing shear at $t_0 = 0.01$, 1 and $t_0 \to \infty$ with neutral waves: (*a*) neutral curves; (*b*) growth rates at $La^{-1} = 5$.

permits us to consider and compare several credible scenarios, beginning with the case of developing shear in the presence of neutral waves. In all cases the flow is non-stratified (i.e. $Ri = 0$).

5.1. *Developing shear with neutral waves*

Here the waves reach maturity well before the substrate, so we let $\tau_0 \to \infty$ and consider three values of t_0, namely 0.01, 1 and ∞, as shown in figure 3(*a*). This case was first investigated by LP who found, in accord with figure 3(*a*), that the least stable situation occurs in the limit $t_0 \to \infty$. Of course we might reasonably question whether the growth rates close to these boundaries are large enough to convey meaningful

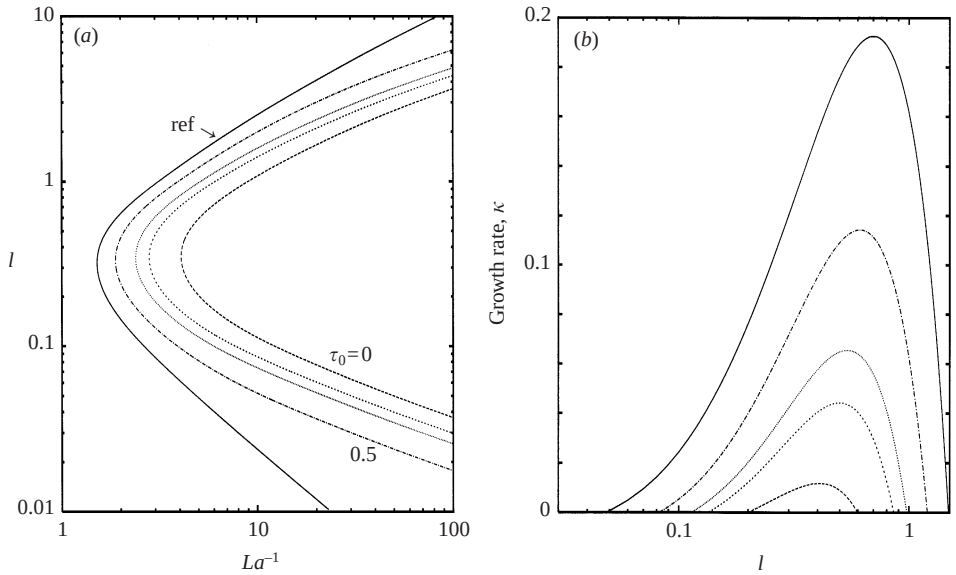

FIGURE 4. Developed shear ($t_0 \to \infty$) with growing waves at $\tau_0 = 0$, 0.2, 0.3, 0.5: (a) neutral curves; (b) growth rates at $La^{-1} = 5$.

information, and to resolve that question we plot the largest positive eigenvalue κ at l_{c0} (see below) for the latter two cases in figure 3(b). It is clear from 3(b) that κ is markedly different in each case and that the case τ_0, $t_0 \to \infty$ is the least stable. Pb further determined that the τ_0, $t_0 \to \infty$ curve depicts the least stable neutral curve for the double limit $Pr = Ri = 0$, and so for that reason we use it as a reference in the cases to follow. Note too that onset in the reference case occurs at $l_{c0} = 0.3187$ and $La_{c0}^{-1} = 1.5157$.

Physically the limit $t_0 \to \infty$ means that the full extent of the developing LCs are subjected to uniform shear, in which case we describe the shear as 'developed' or 'mature'. Such usage is of course from the viewpoint of the instability, because in fact the shear layer grows indefinitely.

5.2. *Developed shear with growing waves*

We now consider the reverse case, in which the substrate reaches maturity prior to the waves. Here the shear is uniform while the waves continue to grow. Neutral curves for this case are plotted in figure 4(a) along with the reference curve, which is of course recovered, as (see figure 2) $\tau_0 \to \infty$. Of particular interest is the case for which D_3 is a maximum ($\tau_0 = 0.2$) which falls to the right of the reference curve. This indicates that growing waves in the presence of uniform shear are stabilizing to the generation of LCs. In fact, of the growing wave cases considered, the least stable is that for $\tau_0 = 0.5$ (at which point $D_1 \approx 2D_3$). The eigenvalues κ shown in figure 4(b) agree. Note too that the spanwise wavenumber at onset at $\tau_0 = 0.5$ is $l_c = 0.3320$; thus since $l_c > l_{c0}$ we infer that growing waves act to increase the onset spanwise wavenumber.

5.3. *Developed shear with decaying waves*

Of course if after some time the wind were to suddenly cease, the waves would then decay in the presence of uniform shear. In this instance, as we see in figure 5(a), the flow is stabilizing to LCs for $l > l_{c0}$ and destabilizing for $l \ll l_{c0}$. Note, however,

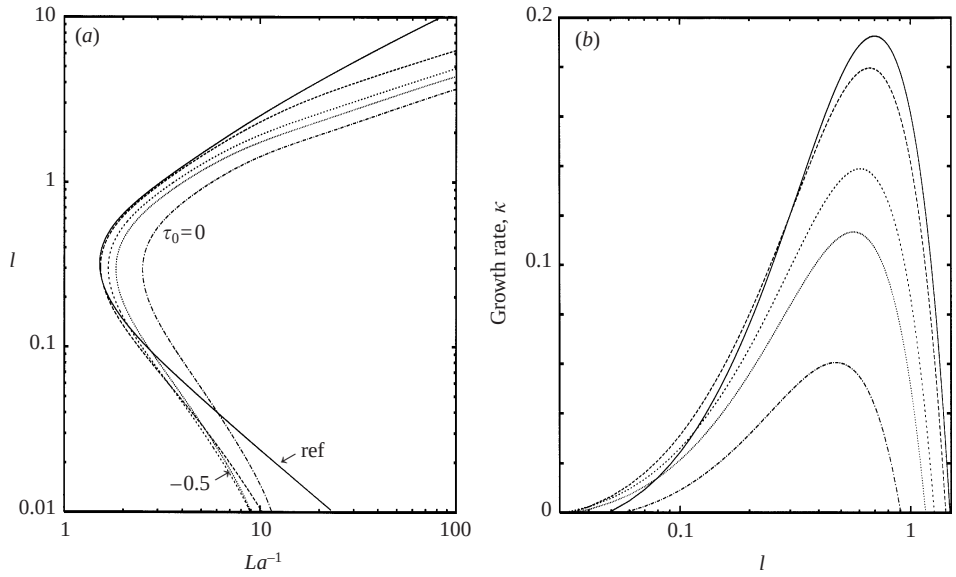

FIGURE 5. Developed shear ($t_0 \to \infty$) with decaying waves at $\tau_0 = -0.5, -0.3, -0.2, 0$: (*a*) neutral curves; (*b*) growth rates at $La^{-1} = 5$.

that La_c^{-1} at all times exceeds the global lower bound of 1.4395 for non- or stably stratified flow reported by LP and that the maximum growth rate occurs in the stabilizing wavenumber range, as we see in figure 5(*b*). The interaction is also slightly stabilizing at onset for $\tau_0 = -0.5$, where, compared with La_{c0}^{-1}, we have $La_c^{-1} = 1.5418$. Furthermore $l_c = 0.3063$ here, suggesting that decaying waves act to decrease the spanwise wavenumber at onset. Finally, we note that contrary to the above cases for growing or neutral waves, which are unstable only for wavenumbers $l > 0$, the case with decaying waves is unstable even in the limit (not shown) $l \to 0$, albeit at $La_c^{-1} \gg La_{c0}^{-1}$.

5.4. *Developing shear with growing waves*

We turn now to the case in which neither the shear nor the waves are mature. Interestingly, although the interaction is stable to the formation of LCs when $t_0 = 0.01$ for $\tau_0 \in [-1, 0.5]$, it is unstable to LCs at $\tau_0 = 1$, as we see in figure 6. Since $D_1 \gg D_3$ when $\tau_0 = 1$ it is evident that the stabilizing effect of growing waves (through D_3) can be overcome by D_1 to drive the instability, even when the shear layer is thin (i.e. the e-folding depth is $\ll 1$). Note, however, that LCs form only for spanwise wavenumbers larger than l_{c0}, and thus that there is a long-wave cutoff.

For more developed shear on the other hand, i.e. $t_0 = 1$, the flow is unstable to LCs at all τ_0, albeit for a restricted range of l; this case is shown in figure 7. Here, in accord with our earlier findings for growing waves, the flow is stabilizing to the formation of LCs and onset occurs at spanwise wavenumbers in excess of l_{c0}.

5.5. *Developing shear with decaying waves*

On the other hand developing shear, which can occur in the absence of wind owing to the wave-induced surface stress of decaying waves, is unstable to LCs for all τ_0 considered at both $t_0 = 0.01$ and $t_0 = 1$, as we see in figures 8 and 9. But comparison of these figures with figure 5 shows that developing shear is stabilizing

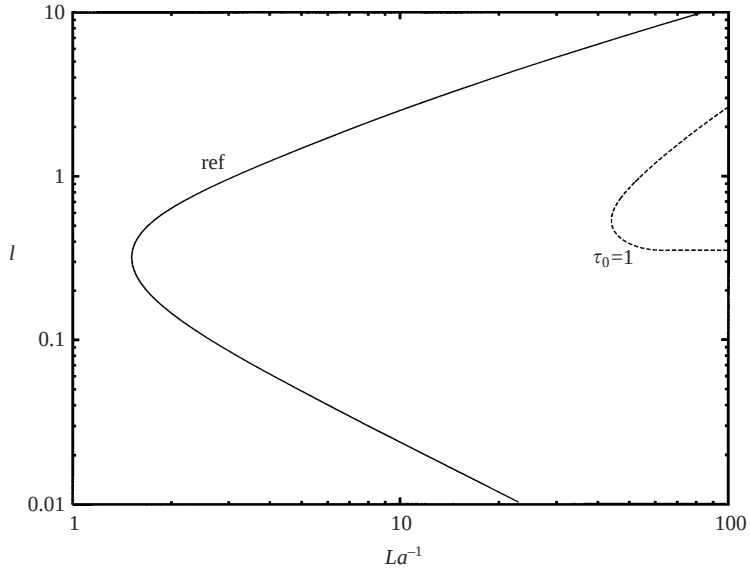

FIGURE 6. Neutral curves for developing shear at $t_0 = 0.01$ with growing waves at $\tau_0 = 1$. Note that the flow is stable to the formation of LCs for $\tau_0 \in [-1, 0.5]$.

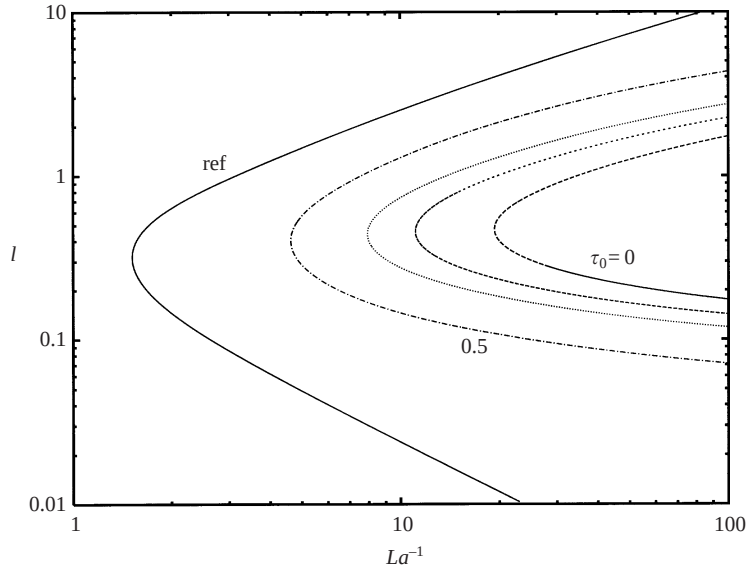

FIGURE 7. Neutral curves for developing shear at $t_0 = 1$ with growing waves at $\tau_0 = 0, 0.2, 0.3, 0.5$.

to the formation of LCs, at least for $l > 0.05$. Not surprisingly the case $t_0 \to \infty$ is the least, and $t_0 = 0.01$ the most, stabilizing, with the implication that the flow is stable to the formation of LCs in the limit $t_0 \to 0$, i.e. in the absence of shear, as it must be.

6. Opposed wind and waves

We now consider the situation in which the wind and waves propagate in opposite directions. Physically this situation might arise if the waves are a result of some distant

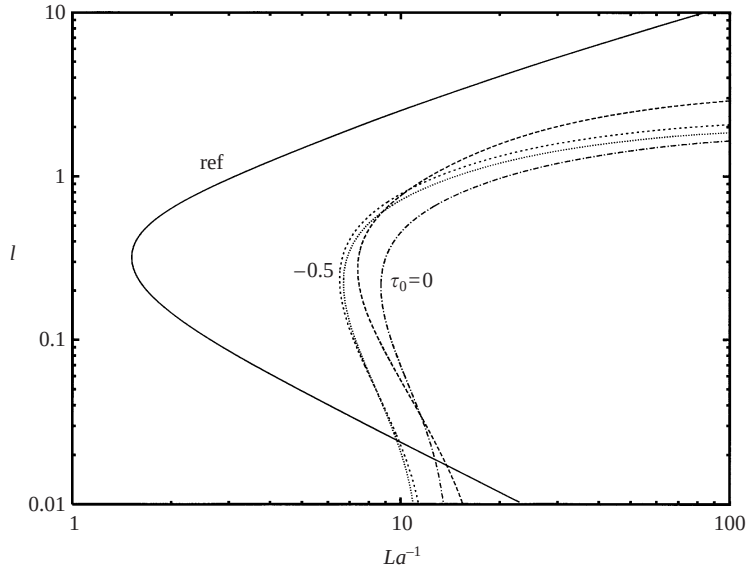

FIGURE 8. Neutral curves for developing shear at $t_0 = 0.01$ with decaying waves at $\tau_0 = -0.5, -0.3, -0.2, 0$.

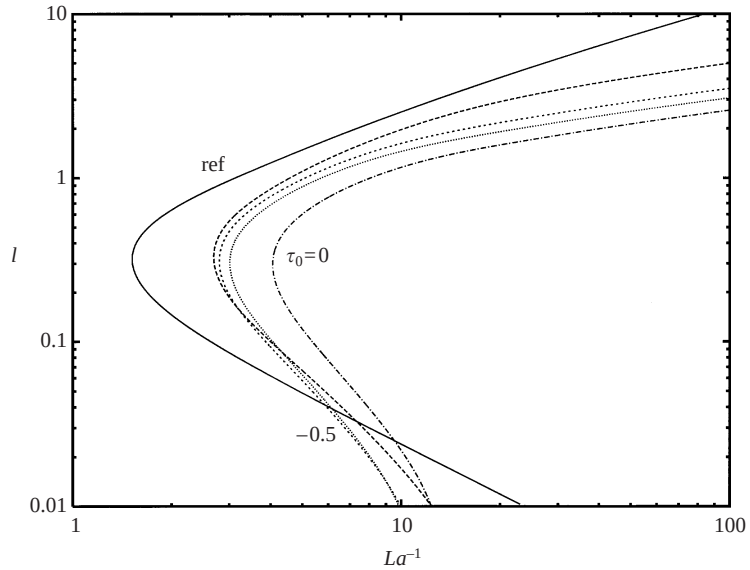

FIGURE 9. Neutral curves for developing shear at $t_0 = 1$ with decaying waves at $\tau_0 = -0.5, -0.3, -0.2, 0$.

weather event, while local winds of increasing strength oppose them. Their respective stresses are thus opposite, but we take the view that their vector sum is, as before, constant. Thus, since u_* is by definition aligned in the x-direction, the magnitude of the wind stress must necessarily exceed the magnitude of the free-surface wave stress, so that the mean Eulerian shear flow is counter to the streamwise component of Stokes drift. Decaying, albeit steepening waves are therefore physically intuitive.

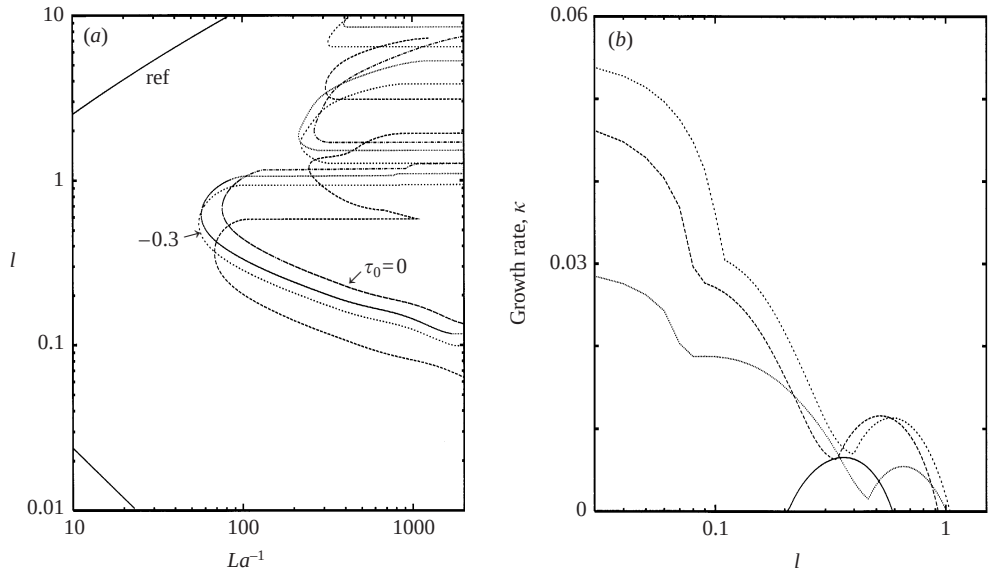

FIGURE 10. Developed shear ($t_0 \to \infty$) with opposed decaying waves at $\tau_0 = -0.5, -0.3, -0.2, 0$: ($a$) neutral curves for stationary solutions; (b) growth rates at $La^{-1} = 100$ for both stationary and convective solutions.

Interestingly, we find the flow is unstable to LCs only if the waves are decaying, as we see in §§ 6.1, 6.2. Here the substrate is also neutrally stratified (so $Ri = 0$).

6.1. *Developed shear with decaying waves*

We look first at figure 10(a) and observe that the flow is least stable when $\tau_0 = -0.3$, at which point $D_1 \approx -D_3$. Observe too that the neutral curves are vastly different from the single elbow form of their coflowing counterparts. Rather, the neutral curves are here fingered, with bands of l that are unstable to LCs and bands that are stable; also the onset La^{-1} far exceeds La_{c0}^{-1}. Notice though, that the bands blend into each other as the waves evolve with τ_0. These (figure 10a) curves are, however, for stationary solutions: indeed, looking at figure 10(b), which is a trace of κ at $La^{-1} = 100$, we see that the flow is in fact unstable to LCs at wavenumbers $l \ll 1$. This instability, however, is associated with convective solutions which have noticeably higher growth rates than their stationary counterparts. Interestingly, Pb also observed convective solutions, but only for $Ri \neq 0$; here, however, $Ri = 0$.

6.2. *Developing shear with decaying waves*

Much the same features occur as the substrate grows, although, in accord with our earlier findings, the case with fully developed shear is the least stable, as we see by comparing figures 10, 11 and 12. Also evident is a region of instability for $l \ll 1$. This is the least stable finger and continues to the long-wave limit $l \to 0$; this finger is also present with developed shear but is outside the plotted range.

7. The role of stratification

Pb considers the formation of LCs in the presence of neutral waves and stratification over a wide range of Pr and Ri and finds, *inter alia*, that CL2 is destabilized by diminishing Pr, and thus that LCs can be absent or present at the same La. He

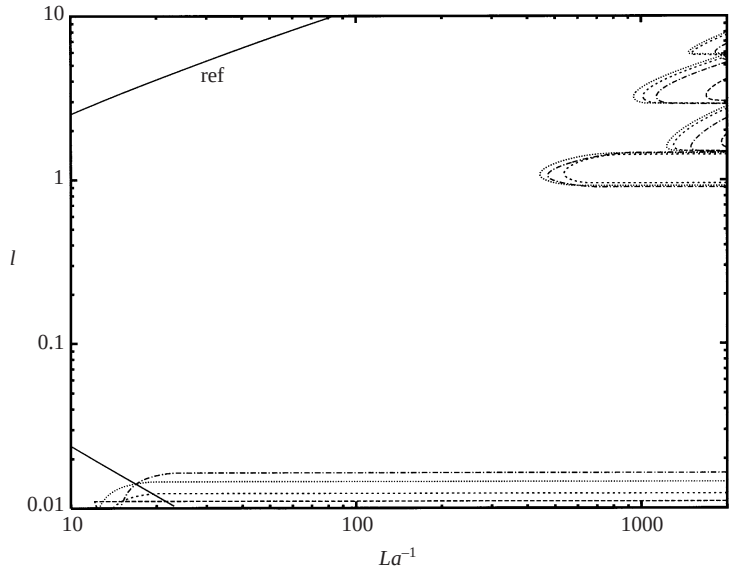

FIGURE 11. Neutral curves for developing shear at $t_0 = 0.01$ with opposed decaying waves at $\tau_0 = -0.5, -0.3, -0.2, 0$.

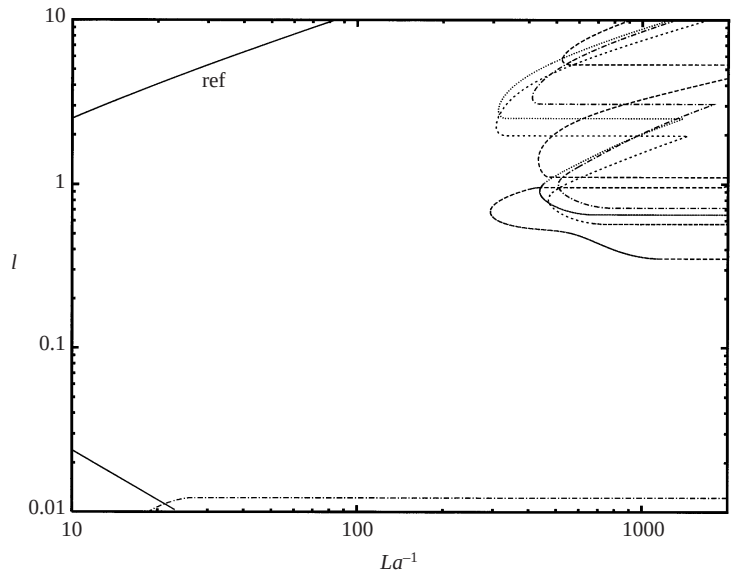

FIGURE 12. Neutral curves for developing shear at $t_0 = 1$ with opposed decaying waves at $\tau_0 = -0.5, -0.3, -0.2, 0$.

further finds that although CL2 is subject to a global lower bound in La^{-1}, La_G^{-1} say, which is independent of Pr and Ri for stabilizing Ri, that is not the case for destabilizing Ri, where La_G^{-1} may diminish to zero. Our intent here is to ascertain the role of stratification on the instability in the presence of temporal waves. In view of the wide parameter range, however, we choose representative values of Prandtl and Richardson numbers, $Pr = 6.7$ and $Ri = \pm 0.1$. We further choose the least stable base flow ($t_0 \to \infty$) and the least stable case for growing ($\tau_0 = 0.5$) and decaying

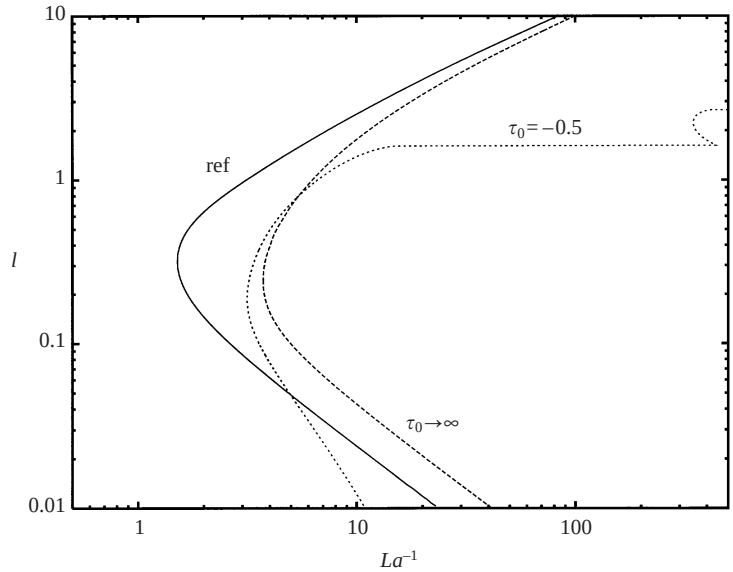

FIGURE 13. Neutral curves for developed stably stratified shear ($t_0 \to \infty$, $Ri = 0.1$ and $Pr = 6.7$), with neutral ($\tau_0 \to \infty$) and decaying ($\tau_0 = -0.5$) waves: note that this configuration is stable to growing waves.

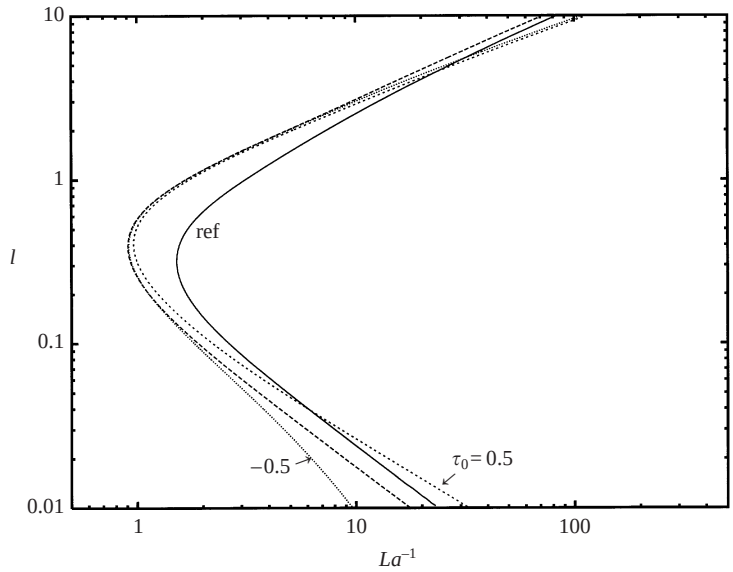

FIGURE 14. Neutral curves for developed unstably stratified shear ($t_0 \to \infty$, $Ri = -0.1$ and $Pr = 6.7$) with growing ($\tau_0 = 0.5$), neutral ($\tau_0 \to \infty$) and decaying ($\tau_0 = -0.5$) waves.

($\tau_0 = -0.5$) waves. These cases are plotted in figures 14, 15 and 16. Finally, in view of our discussion in § 4.2, we here limit our results to the linear steady states.

7.1. *Aligned wind and waves*

Consider first stable stratification ($Ri > 0$). Here we find that growing waves aligned with the wind are stable to the formation of LCs, while neutral and decaying waves are

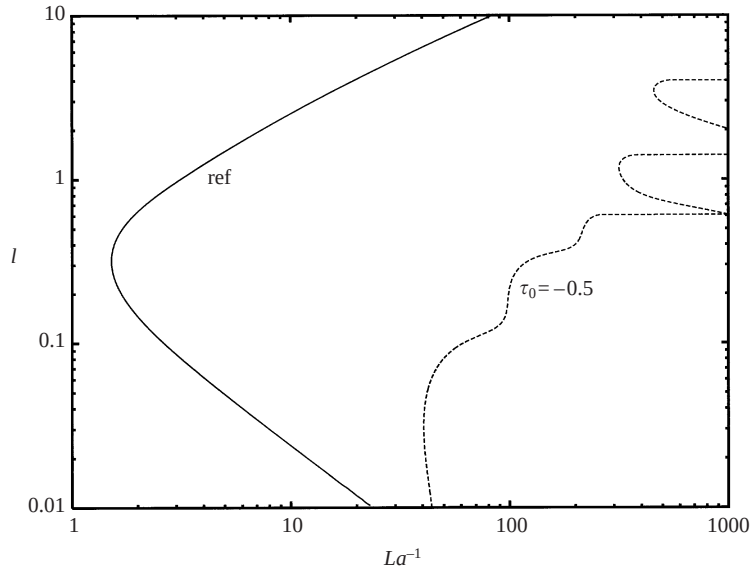

FIGURE 15. Neutral curves for developed stably stratified shear ($t_0 \to \infty$, $Ri = 0.1$ and $Pr = 6.7$) with opposed decaying waves ($\tau_0 = -0.5$). Note that this configuration is stable to neutral and growing waves.

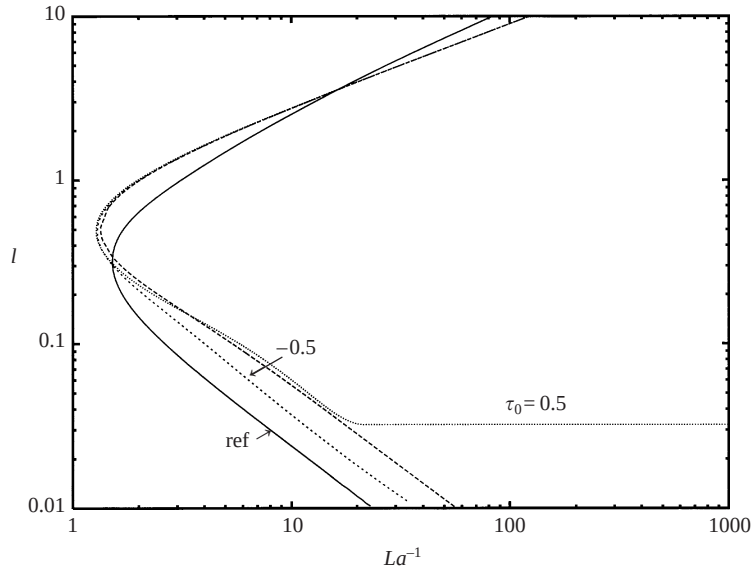

FIGURE 16. Neutral curves for developed unstably stratified shear ($t_0 \to \infty$, $Ri = -0.1$ and $Pr = 6.7$) with opposed growing ($\tau_0 = 0.5$), neutral ($\tau_0 \to \infty$) and decaying ($\tau_0 = -0.5$) waves.

unstable to LCs. Furthermore, while both cases are stabilizing relative to the reference case, decaying waves are destabilizing relative to neutral waves (for $Ri = 0.1$), at least for $l < 1$, as we see in figure 13. Note too that the curve for decaying waves depicts a fingered pattern reminiscent of its counterparts in § 6, although here the fingers are connected.

In unstably stratified ($Ri < 0$) conditions on the other hand, growing, neutral and

decaying waves are unstable to the formation of LCs and destabilizing relative to the reference flow, as we see in figure 14. Moreover, relative to the case of neutral waves at $Ri = -0.1$, and in accord with our earlier findings, decaying waves are destabilizing, at least for $l < 0.1$, and growing waves stabilizing.

7.2. *Opposed wind and waves*

Finally, only decaying waves are destabilizing to LCs when the wind and waves are opposed and the flow is stably stratified, as we see in figure 15. On the other hand, all waves are destabilizing to LCs when the flow is unstably stratified. Note, however, that in this instance growing waves are destabilizing and decaying waves stabilizing relative to the neutral wave case at $Ri = -0.1$. Furthermore, decaying waves depict a long-wave cutoff, as we see in figure 16.

8. Discussion

Nature is hostage neither to theory nor the constraints of field observations. So in comparing our theory with observations of wind, waves and LCs, we should be aware of a plethora of additional variables: internal waves, thermoclines, swells from afar, variations in mixed layer depth and more, which occur in Nature, but which are not considered in the theory. Nevertheless, it remains instructive to compare what we know from theory with what we know from field observations.

At the onset of a wind event after a quiescent period there would presumably be developing shear and growing waves, with an associated tendency for the instability to occur at relatively high wavenumber (figures 6 and 7). If the shear reaches full development while waves are still growing (which seems plausible), then the unstable wavenumber is near l_{c0} (figure 4). Unless the wind drops very slowly, the wave field will decay more slowly than the (wind-driven) shear, and the instability will move to lower wavenumber (figure 5).

At the risk of reading too much into these idealized results, we can relate this sequence of events to observations of LC evolution during the Surface Waves Processes Program (Plueddemann *et al.* 1996; Plueddemann 2001, private communication). Here the most energetic LCs tend to be small at the onset of a wind event and achieve their maximum size (which seems to be limited by the mixed layer depth) at about the time the wave field matures. Moreover decaying wave fields apparently continue to 'force' the largest LCs, which accounts for the observation of LCs persisting after a dramatic drop in wind speed. But it is not clear whether only the largest scales persist and thus a careful study of the variability of LC scales during wind–wave events is warranted. Also unclear is how the relative growth rates and wave age (as used here; see § 4.4) can be estimated during an event, and thus directly related to the theory. Nevertheless the similarities between the theory and observation are striking, particularly in the light of Pb's recent finding that CL2 can also credibly explain some of Smith's (1992) observations.

But how is the instability influenced by temporal waves? As noted above, CL2 occurs because the differential Stokes drift $\mathrm{D}D_1$ causes vortex lines to tilt forward wherever the Eulerian mean shear is distorted in y, giving rise to a longitudinal component of vorticity and ultimately vortices. Here we find that temporal waves, through the gradient $\mathrm{D}D_3$, act to further advect vortex lines, but up or down (i.e. in z) according to whether the waves are growing or decaying, thereby increasing or decreasing the z-gradient of streamwise vorticity and, in turn, the rate at which the instability grows.

That rate, as we saw in § 3, can be doubly exponential in time. This, of course, does not mean a change in time scale (for the formation of LCs) from tens of minutes to minutes, but it does mean that LCs in growing waves are more vigorous (intense) at a given time after onset than their counterparts in decaying waves, a feature that should be clear from an observational viewpoint. Finally we note that examples of wavy shear flows that are unstable to doubly exponentially growing longitudinal vortices are rare, to our knowledge the only other example being in Wu (1993).

I should like to thank Greg Chini, Alex Craik and Al Plueddemann for their interest and helpful comments. The work was supported by the National Science Foundation through OCE grants 9818092 and 0116921.

REFERENCES

Andrews, D. G. & McIntyre, M. E. 1978 An exact theory of nonlinear waves on a Lagrangian-mean flow. *J. Fluid Mech.* **89**, 609–646.

Baines, P. G. & Gill, A. E. 1969 On thermohaline convection with linear gradients. *J. Fluid Mech.* **37**, 289–306.

Brown, S. N. & Stewartson, K. 1965 Laminar separation. *Annu. Rev. Fluid Mech.* **1**, 45–72.

Cox, S. M. & Leibovich, S. 1993 Langmuir circulations in a surface layer bounded by a strong thermocline. *J. Phys. Oceanogr.* **23**, 1330–1345.

Cox, S. M. & Leibovich, S. 1997 Large-scale three-dimensional Langmuir circulation. *Phys. Fluids* **9**, 2851–2863.

Cox, S. M., Leibovich, S., Moroz, I. M. & Tandon, A. 1992 Non-linear dynamics in Langmuir circulations with $O(2)$ symmetry. *J. Fluid Mech.* **241**, 669–704.

Craik, A. D. D. 1977 The generation of Langmuir circulations by an instability mechanism. *J. Fluid Mech.* **81**, 209–223.

Craik, A. D. D. 1982*a* The drift velocity of water waves. *J. Fluid Mech.* **116**, 187–205.

Craik, A. D. D. 1982*b* The generalized Lagrangian-mean equations and hydrodynamic stability. *J. Fluid Mech.* **125**, 27–35.

Craik, A. D. D. 1982*c* Wave-induced longitudinal-vortex instability in shear layers. *J. Fluid Mech.* **125**, 37–52.

Craik, A. D. D. & Leibovich, S. 1976 A rational model for Langmuir circulations. *J. Fluid Mech.* **73**, 401–426.

Drazin, P. G. & Reid, W. H. 1981 *Hydrodynamic Stability*. Cambridge University Press.

Foster, T. D. 1965 Stability of homogeneous fluid cooled uniformly from above. *Phys. Fluids* **8**, 1249–1257.

Gargett, A. E. 1989 Ocean turbulence. *Annu. Rev. Fluid Mech.* **21**, 419–451.

Homsy, G. M. 1973 Global stability of time dependent flows: impulsively heated or cooled liquid layers. *J. Fluid Mech.* **60**, 129–139.

Kenney, B. C. 1993 Observations of coherent bands of algae in a surface shear layer. *Limnol. Oceanogr.* **38**, 1059–1067.

Langmuir, I. 1938 Surface motion of water induced by wind. *Science* **87**, 119–123.

Leibovich, S. 1977 Convective instability of stably stratified water in the ocean. *J. Fluid Mech.* **82**, 561–585.

Leibovich, S. 1980 On wave-current interaction theories of Langmuir circulations. *J. Fluid Mech.* **99**, 715–724.

Leibovich, S. 1983 The form and dynamics of Langmuir circulations. *Annu. Rev. Fluid Mech.* **15**, 391–427.

Leibovich, S., Lele, S. & Moroz, I. M. 1989 Nonlinear dynamics in Langmuir circulations and thermosolutal convection. *J. Fluid Mech.* **198**, 471–511.

Leibovich, S. & Paolucci, S. 1980 Energy stability of the Eulearian-mean motion in the upper ocean to three-dimensional perturbations. *Phys. Fluids* **23**, 1286–1290.

Leibovich, S. & Paolucci, S. 1981 The instability of the ocean to Langmuir circulations. *J. Fluid Mech.* **102**, 141–167 (referred to herein as LP).

Li, M. & Garrett, C. 1993 Cell merging and the jet/downwelling ratio in Langmuir circulation. *J. Mar. Res.* **51**, 737–769.

Li, M. & Garrett, C. 1997 Mixed layer deepening due to Langmuir circulation. *J. Phys. Oceanogr.* **27**, 121–132.

Li, M., Zahariev, K. & Garrett, C. 1995 Role of Langmuir circulation in the deepening of the ocean surface mixed layer. *Science* **270**, 1955–1957.

Longuet-Higgins, M. S. 1953 Mass transport in water waves. *Phil. Trans. R. Soc. Lond.* A **245**, 535–581.

McIntyre, M. E. 1988 A note on the divergence effect and the Lagrangian-mean surface elevation in periodic water waves. *J. Fluid Mech.* **189**, 235–242.

McIntyre, M. E. & Norton, W. A. 1990 Dissipative wave-mean interactions and the transport of vorticity or potential vorticity. *J. Fluid Mech.* **212**, 403–435.

McWilliams, J. C., Sullivan, P. P. & Moeng, C.-H. 1997 Langmuir circulations in the ocean. *J. Fluid Mech.* **334**, 1–30.

Melville, W. K., Shear, R. & Veron, F. 1998 Laboratory measurements of the generation and evolution of Langmuir circulations. *J. Fluid Mech.* **364**, 31–58.

Phillips, W. R. C. 1996 On a class of unsteady boundary layers of finite extent. *J. Fluid Mech.* **319**, 151–170.

Phillips, W. R. C. 1998 Finite amplitude rotational waves in viscous shear flows. *Stud. Appl. Maths* **101**, 23–47 (referred to herein as P98).

Phillips, W. R. C. 2001*a* On the pseudomomentum and generalized Stokes drift in a spectrum of rotational waves. *J. Fluid Mech.* **430**, 209–229 (referred to herein as Pa).

Phillips, W. R. C. 2001*b* On an instability to Langmuir circulations and the role of Prandtl and Richardson numbers. *J. Fluid Mech.* **442**, 335–358 (referred to herein as Pb).

Phillips, W. R. C. 2003 Langmuir circulations. In *Surface Waves* (ed. J. C. R. Hunt & S. G. Sajjadi), p. 10. Oxford University Press (to appear).

Phillips, W. R. C. & Wu. Z. 1994 On the instability of wave-catalysed longitudinal vortices in strong shear. *J. Fluid Mech.* **272**, 235–254.

Phillips, W. R. C., Wu. Z. & Lumley, J. L. 1996 On the formation of longitudinal vortices in turbulent boundary layers over wavy terrain. *J. Fluid Mech.* **326**, 321–341.

Plueddemann, A. J., Smith, J. A., Farmer, D. M., Weller, R. A., Crawford, W. R., Pinkel, R., Vagle, S. & Gnanadesikan, A. 1996 Structure and variability of Langmuir circulation during the Surface Waves Processes Program. *J. Geophys. Res.* **101**, 3525–3543.

Plueddemann, A. J. & Weller, R. A. 1999 Structure and evolution of the oceanic surface boundary layer during the Surface Waves Processes Program. *J. Mar. Syst.* **21**, 85–102.

Skyllingstad, E. D. & Denbo, D. W. 1995 An ocean large eddy simulation of Langmuir cells and convection in the surface mixed layer. *J. Geophys. Res.* **100**, 8501–8522.

Smith, J. A. 1992 Observed growth of Langmuir circulation. *J. Geophys. Res.* **97**, 5651–5664.

Smith, J. A. 1998 Evolution of Langmuir circulation in a storm. *J. Geophys. Res.* **103**, 12649–12668.

Smith, J., Pinkel, R. & Weller, R. A. 1987 Velocity structure in the mixed layer during MILDEX. *J. Phys. Oceanogr.* **17**, 425–439.

Thorpe, S. A. & Hall, A. J. 1982 Observations of the thermal structure of Langmuir circulation. *J. Fluid Mech.* **114**, 237–250.

Weller, R. A., Dean, J. P., Marra, J., Price, J. F., Francis, E. A. & Broadman, D. C. 1985 Three-dimensional flow in the upper ocean. *Science* **227**, 1552–1556.

Weller, R. A. & Plueddemann, A. J. 1996 Observations of the vertical structure of the oceanic boundary layer. *J. Geophys. Res.* **101**, 3525–3543.

Weller, R. A. & Price, J. F. 1988 Langmuir circulation within the oceanic mixed layer. *Deep-Sea Res.* **35**, 711–747.

Wu, X. 1993 Nonlinear temporal-spatial modulation of near planar Rayleigh waves in shear flows: formation of streamwise vortices. *J. Fluid Mech.* **256**, 685–719.

Zedel, L. & Farmer, D. 1991 Organized structures in subsurface bubble clouds: Langmuir circulation in the upper ocean. *J. Geophys. Res.* **96**, 8889–8900.